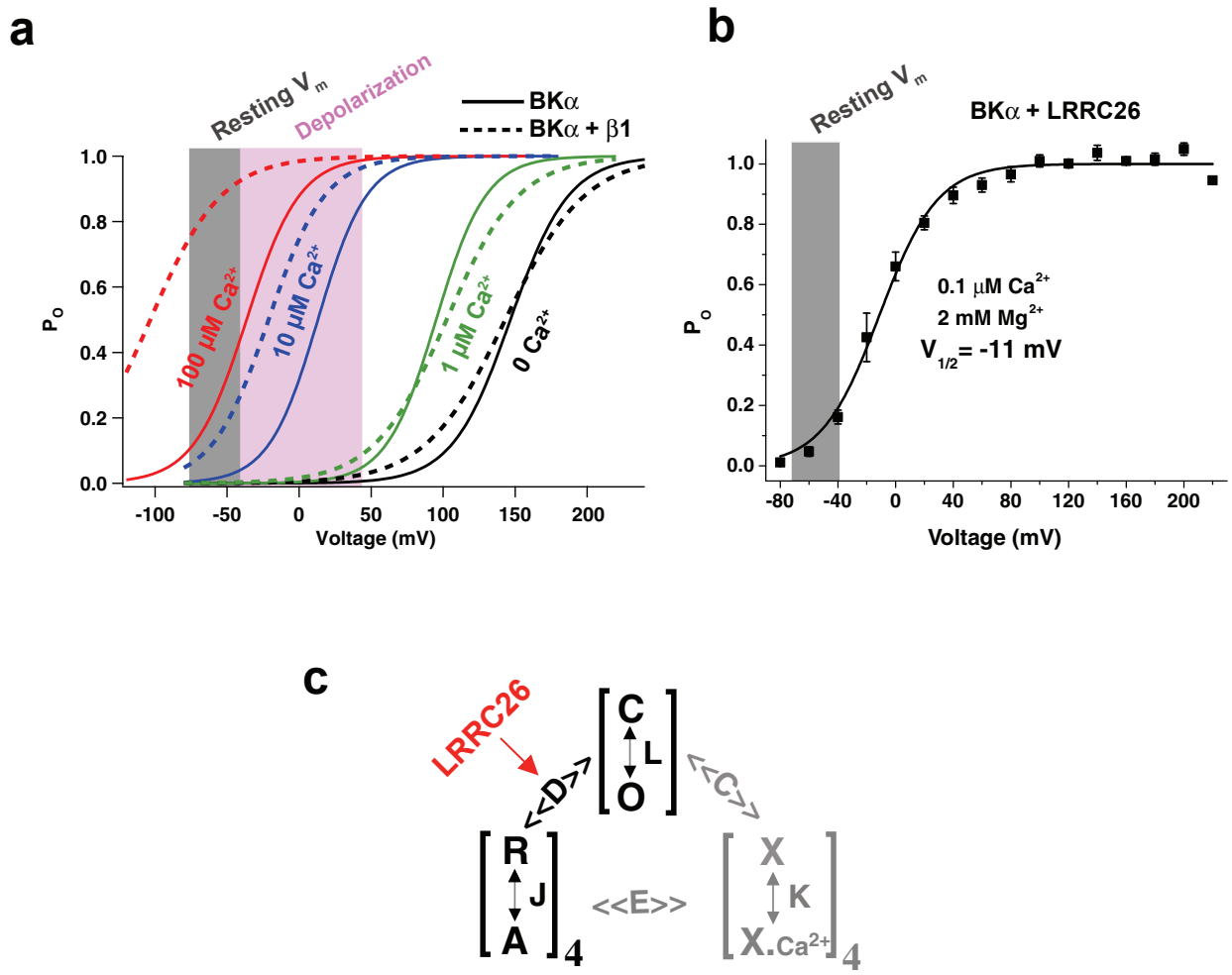

Supplementary Figure 1

Summary of the background and main findings. a, Representative P_o-voltage curves of human BKα with (dotted lines) or without (solid lines) β1 subunit transiently expressed in HEK-293 cells. Note: without significant increase in $[Ca^{2+}]_{in}$ (> 1 μM), BK channels are barely open in physiological voltage range (resting or depolarized condition). **b**, LRRC26-associated BK channel complex in LRRC26-transfected PC-3 cells can open to a significant level (P_o = ~0.2 at -40 mV) at near physiological condition: 2 mM $[Mg^{2+}]_{in}$ and 100 nM $[Ca^{2+}]_{in}$ ($V_{1/2}$= -11 ± 4 mV, z=1.43 ± 0.16 *e*, n=5). **c**, LRRC26 mainly affects the allosteric coupling (D) between the voltage sensor activation and the channel opening.

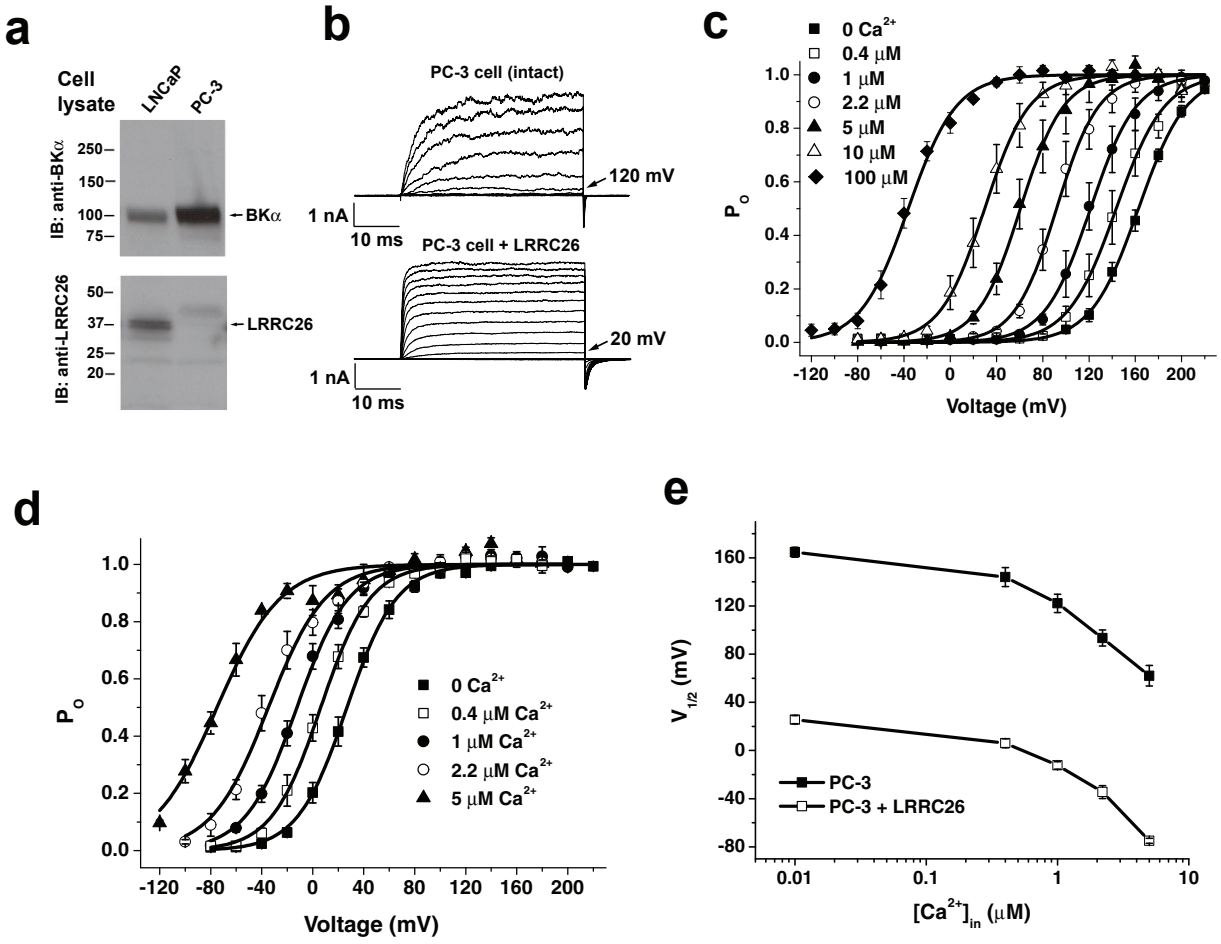

Supplementary Figure 2

Properties of BK channels in PC-3 cells with and without LRRC26-transfection .

a, Immunoblots of BKα and LRRC26 in detergent solubilized cell lysates of LNCaP and PC-3 cells. Each lane was loaded with same amount of total protein. **b**, K^+ currents of BK channels recorded at 0 $[Ca^{2+}]_{in}$ in excised inside-out patches of PC-3 cells with and without LRRC26-transfection. K^+ currents were recorded in response to depolarization of membrane potential from -80 mV in 20 mV step. **c**, P_o-voltage relations of BK channels in untransfected PC-3 cells at different $[Ca^{2+}]_{in}$ conditions: 0 $[Ca^{2+}]_{in}$ ($V_{1/2}$=162 ± 3 mV, z=1.31 ± 0.08 *e*, n=8), 0.4 μM $[Ca^{2+}]_{in}$ ($V_{1/2}$=144 ± 8 mV, z=1.37 ± 0.10 *e*, n=4), 1.0 μM $[Ca^{2+}]_{in}$ ($V_{1/2}$=122 ± 8 mV, z=1.45 ± 0.16 *e*, n=4), 2.2 μM $[Ca^{2+}]_{in}$ ($V_{1/2}$=93 ± 7 mV, z=1.62 ± 0.28 *e*, n=4), 5.0 μM $[Ca^{2+}]_{in}$ ($V_{1/2}$=62 ± 9 mV, z=1.49 ± 0.23 *e*, n=3), 10 μM $[Ca^{2+}]_{in}$ ($V_{1/2}$=31 ± 8 mV, z=1.46 ± 0.14 *e*, n=4), and 100 μM $[Ca^{2+}]_{in}$ ($V_{1/2}$=-36 ± 4 mV, z=1.27 ± 0.09 *e*, n=4). **d**, P_o-voltage relations of BK channels in LRRC26-transfected PC-3 cells at different $[Ca^{2+}]_{in}$ conditions: 0 $[Ca^{2+}]_{in}$ ($V_{1/2}$=26 ± 3 mV, z=1.47 ± 0.11 *e*, n=12), 0.4 μM $[Ca^{2+}]_{in}$ ($V_{1/2}$=6 ± 4 mV, z=1.39 ± 0.07 *e*, n=5), 1.0 μM $[Ca^{2+}]_{in}$ ($V_{1/2}$=-12 ± 3 mV, z=1.33 ± 0.10 *e*, n=5), 2.2 μM $[Ca^{2+}]_{in}$ ($V_{1/2}$=-34 ± 5 mV, z=1.25 ± 0.15 *e*, n=4), and 5.0 μM $[Ca^{2+}]_{in}$ ($V_{1/2}$=-75 ± 2 mV, z=1.05 ± 0.16 e, n=3). **e**, Plots of $V_{1/2}$-$[Ca^{2+}]_{in}$ relations for BK channels in PC-3 cells with and without LRRC26-transfection.

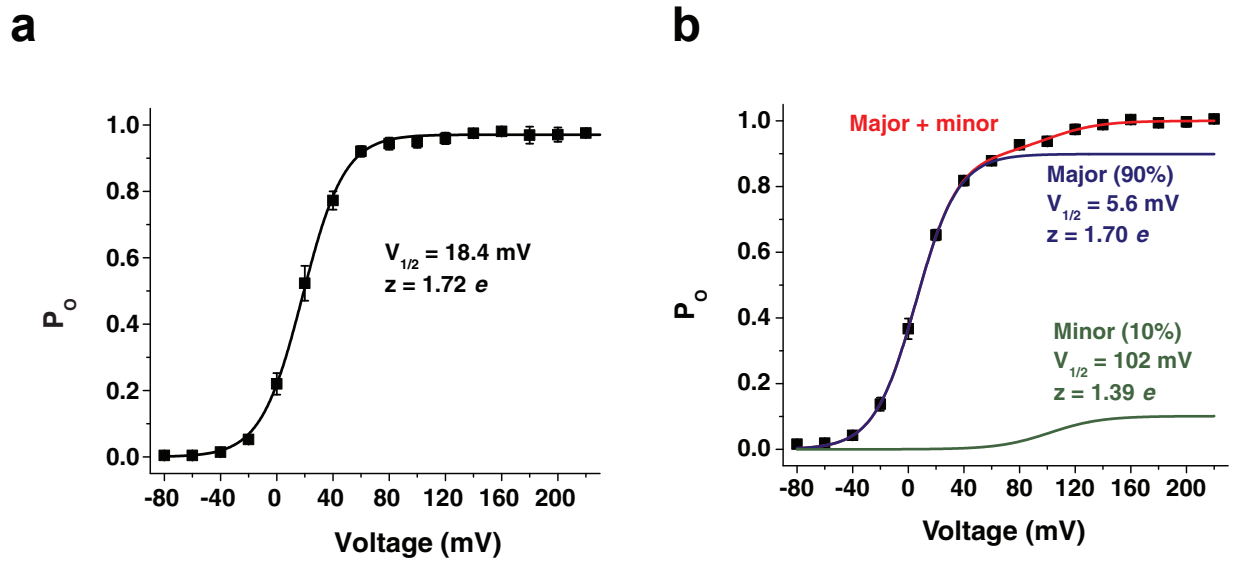

Supplementary Figure 3
Electrophysiological properties of BKα-LRRC26 channel complex in HEK-293 cells.
a, P_o-voltage relation of the BK channels expressed by BKα-LRRC26 fusion construct in HEK-293 cells at 0 $[Ca^{2+}]_{in}$ which was best fitted by a single Boltzmann function.
b, P_o-voltage relation of the BK channels at 0 $[Ca^{2+}]_{in}$ when BKα and LRRC26 were co-expressed separately in HEK-293 cells, which was best fitted by a double Boltzmann function with most channels (90%) having a low $V_{1/2}$ ($V_{1/2}$ = 5.6 mV). The high-$V_{1/2}$ ($V_{1/2}$ = 102 mV) fraction might arise from channels associated with fewer number (<4) of LRRC26 molecules per channel.
Note: When LRRC26's *N*-terminus is fused to the *C*-terminus of BKα, this BKα-LRRC26 fusion construct might facilitate the formation of a BK channel complex of 4 LRRC26 per channel through cotranslational assembly.

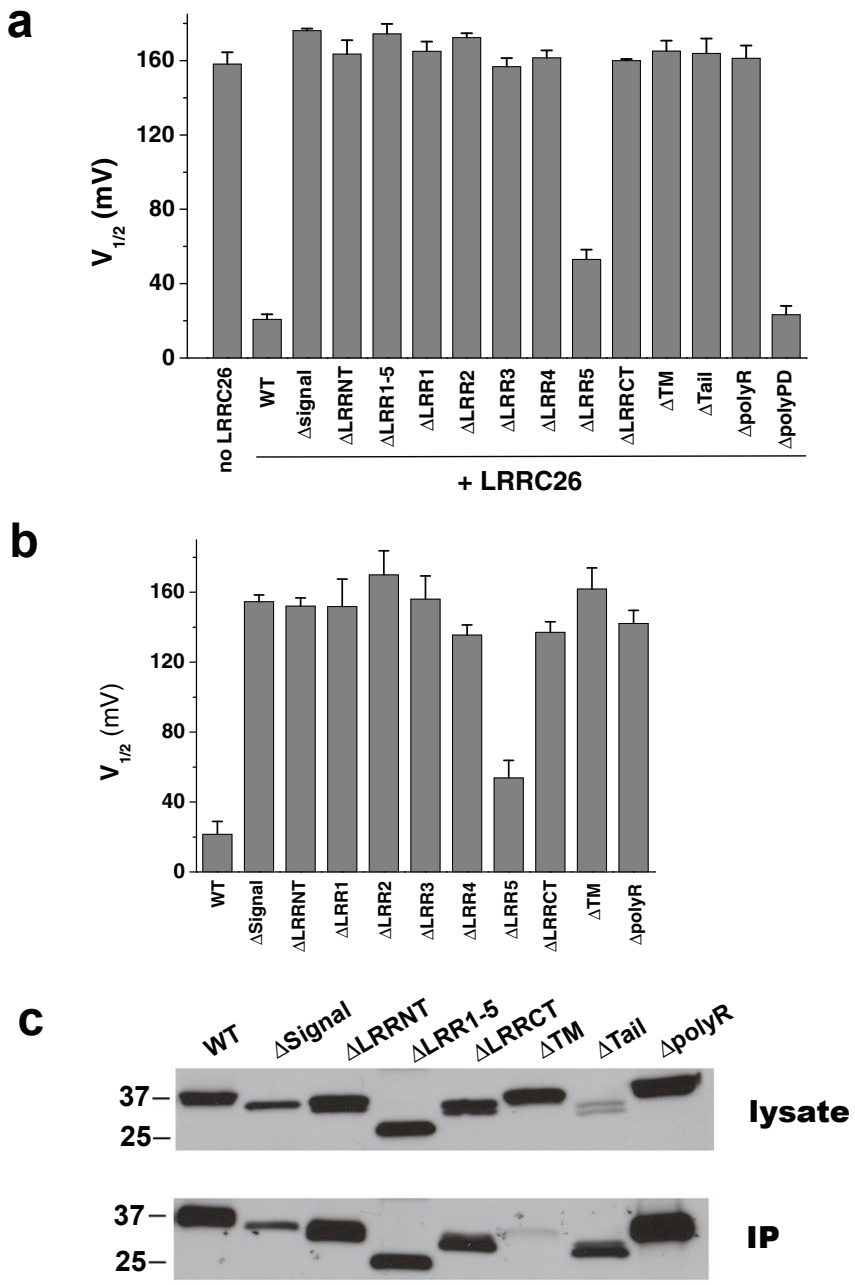

Supplementary Figure 4
Effects of regional deletions on LRRC26's modulatory function.
a, $V_{1/2}$ of BK channels at 0 $[Ca^{2+}]_{in}$ in HEK-293 cells constitutively expressing BKα and transiently expressing LRRC26 WT or deletion mutants (Tail, residues 291-334; polyR, residues 291-298; polyPD, residues 304-316). **b**, $V_{1/2}$ of BK channels at 0 $[Ca^{2+}]_{in}$ expressed in HEK-293 cells by BKα-LRRC26 fusion constructs with regional deletion of LRRC26. **c**, Immunoblot and SDS-PAGE analyses of LRRC26 mutants expression and their binding capabilities to BKα in transfected HEK-293 cells. LRRC26 WT or mutant was transiently expressed in BKα stable expression cell line of HEK-293 cells, extracted by detergent (cell lysate, upper panel), co-immunoprecipitated by anti-BKα antibody (IP, bottom panel), and then probed by anti-myc antibody recognizing myc-tagged recombinant LRRC26 on blot membranes.

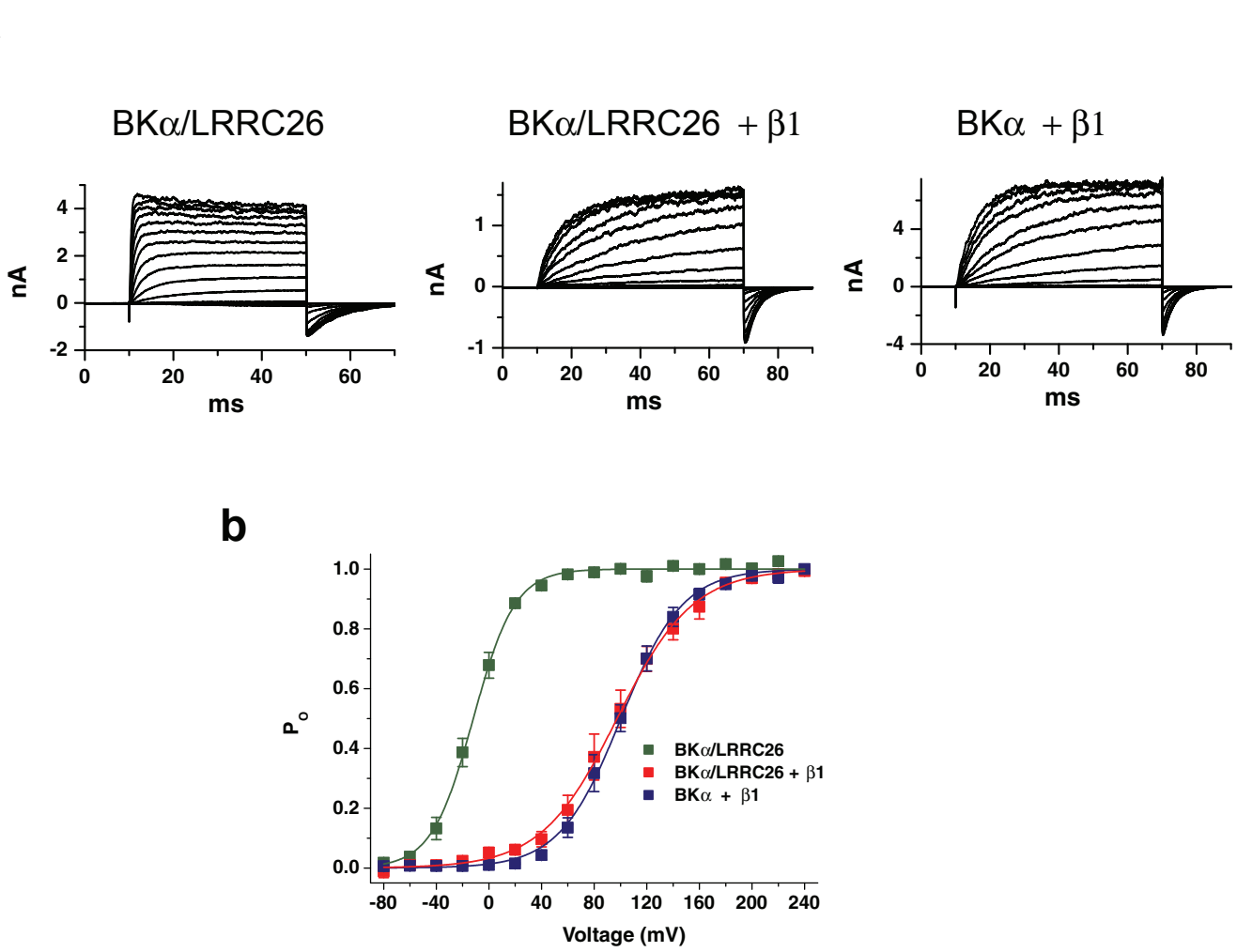

Supplementary Figure 5
Effect of β1 subunit on LRRC26's modulatory function.
K^+ currents (**a**) and the P_o-voltage relations (**b**) of BK channels at 1 μM $[Ca^{2+}]_{in}$ expressed by BKα or BKα-LRRC26 fusion (BKα/LRRC26) constructs in the absence or presence of mouse β1 subunit in HEK-293 cells. Currents were recorded in excised inside-out patches in response to depolarization of membrane potential from -80 mV to 220 mV in 20 mV step.

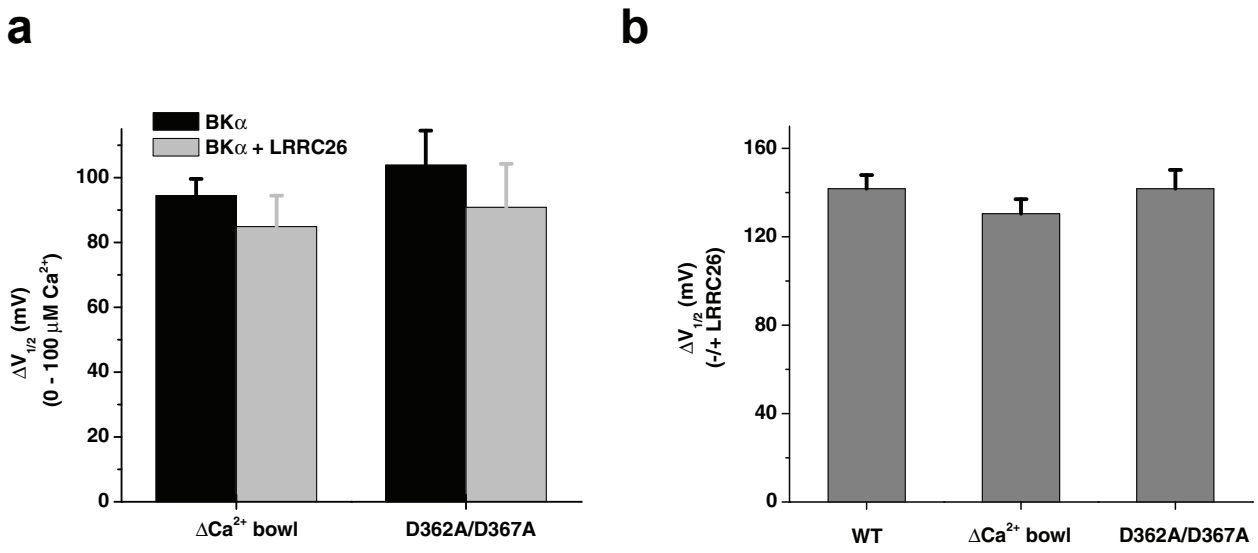

Supplementary Figure 6
Relationship between LRRC26 modulation and the Ca^{2+} activating mechanisms.
a, Shifts in $V_{1/2}$ caused by 100 μM $[Ca^{2+}]_{in}$ for BK channel's Ca^{2+} binding site-deficient mutants at the Ca^{2+}-bowl (ΔCa^{2+}-bowl: residues 893-900) and the RCK1 (D362A/D367A) sites in the absence or presence of LRRC26. **b**, Shifts in $V_{1/2}$ caused by LRRC26 for BK channel's Ca^{2+} binding site-deficient mutants.
Note: The effect of LRRC26 on calcium sensitivity of BK channels was first tested with LRRC26-transfected PC-3 cells up to 5 μM $[Ca^{2+}]_{in.}$ (Supplementary Figure 2), and here BKα mutants which remove Ca^{2+} activation at either the Ca^{2+}-bowl (ΔCa^{2+} bowl) or the RCK1 site (D362A/D367A)[20] were employed to evaluate the calcium sensitivity of BKα-LRRC26 complex at higher $[Ca^{2+}]_{in}$ (100 μM).

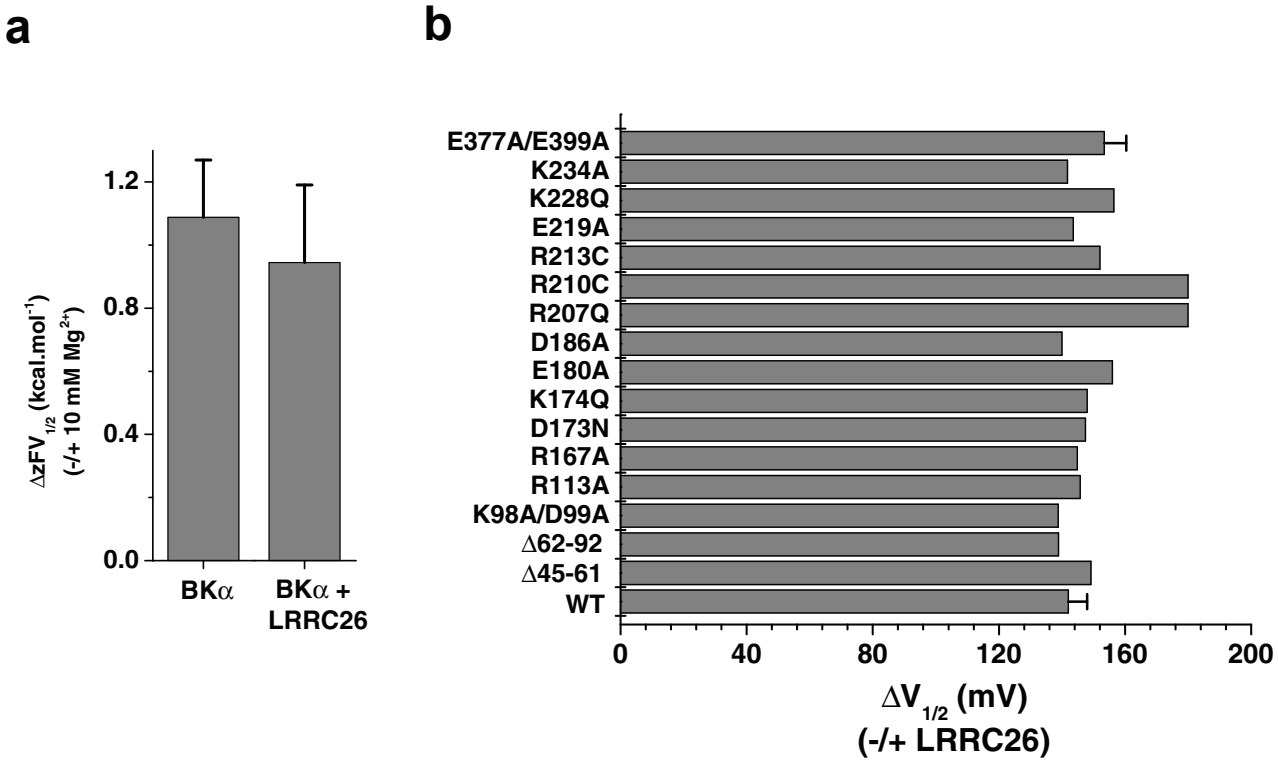

Supplementary Figure 7
Relationship between LRRC26 modulation and the Mg^{2+} activating mechanisms.
a, Free energy provided by Mg^{2+} binding for BKα WT channels in the absence or presence of LRRC26. **b**, Shifts in $V_{1/2}$ caused by LRRC26 for BK channel's Mg^{2+} binding site-deficient mutant (E374A/E399A), and charge neutralization or deletion mutants for charged residues on the intracellular side of the transmembrane domains (S0-S6). R167A and R213C mutants were measured at 10 μM $[Ca^{2+}]_{in}$. Because of the decreased z values, the R207Q and R210C mutants in the presence of LRRC26 were significantly activated at negative voltages up to -200 mV and a roughly estimated $\Delta V_{1/2}$ value for these two mutants was used for plot.
Note: Mg^{2+} activates the BK channels through binding at a site (Glu374 and Glu399) within the RCK1 domain and electrostatically interacts with a charged residue (Arg213) of the voltage sensor domain on the intracellular side[26]. It is shown here that LRRC26 has no significant effect on BK channel's Mg^{2+} sensitivity and neutralization or deletion of the charged residues in Mg^{2+} binding sites or in the intracellular side of the voltage sensor domain has no influence on LRRC26 modulation.